

Nonlinear optical response and spin-charge separation in one-dimensional Mott insulators

Y. Mizuno, K. Tsutsui, T. Tohyama,* and S. Maekawa

Institute for Materials Research, Tohoku University, Sendai 980-8577, Japan

(May 20, 2019)

We theoretically study the nonlinear optical response and photoexcited states of the Mott insulators. The nonlinear optical susceptibility $\chi^{(3)}$ is calculated by using the exact diagonalization technique on small clusters. From the systematic study of the dependence of $\chi^{(3)}$ on dimensionality, we find that the spin-charge separation plays a crucial role in enhancing $\chi^{(3)}$ in the one-dimensional (1D) Mott insulators. Based on this result, we propose a *holon-doublon* model, which describes the nonlinear response in the 1D Mott insulators. These findings show that the spin-charge separation will become a key concept of optoelectronic devices.

PACS numbers: 78.20.-e, 78.20.Bh, 42.65.-k, 71.10.Fd

The charge gap in Mott insulators is a consequence of strong electron correlation. This is completely different from the band insulators, where the charge gap is basically originated from band effects. The nature of charge excitation across the gap is thus essentially different between the two types of insulators. The optical response is used to investigate the charge excitation across the gap. In the response, the linear susceptibility with respect to the applied electric field, $\chi^{(1)}$, provides information on the dipole-allowed states with odd parity. In addition to $\chi^{(1)}$, the nonlinear susceptibilities detect the odd states together with the dipole-forbidden states with even parity.¹

Very recently, anomalously enhanced third-order nonlinear optical susceptibility $\chi^{(3)}$ has been reported for one-dimensional (1D) Mott insulators of Cu-oxides and Ni-halides,² as compared with those for the band insulators. In addition, the 1D Cu oxide, Sr_2CuO_3 , exhibits ultrafast nonlinear optical response (~ 1 ps) at room temperature.³ These facts strongly suggest a great potential of the 1D Mott insulators as novel optoelectronic materials with high performance.^{2,3} Furthermore, it is shown that $\chi^{(3)}$ in two-dimensional (2D) Mott insulators is smaller than that in the 1D Mott insulators.⁴

Motivated by these striking experiments, we theoretically examine photoexcited states and nonlinear optical response in the Mott insulators, and clarify underlying physics of optical nonlinearity of the 1D Mott insulators. We use the half-filled Hubbard model to describe the Mott insulators. The $\chi^{(3)}$ is calculated by using the numerically exact diagonalization method on finite-size clusters, and compared with that for higher dimensional systems with ladder and 2D geometry. We find that $\chi^{(3)}$ increases with decreasing the dimensionality. It is shown that in the 1D system dipole-allowed (odd) and -forbidden (even) states are almost degenerate in energy, having very large dipole coupling between the two states, while in the 2D system the dipole coupling is rather small in spite of closeness of the odd and even states. We demonstrate that this peculiar feature in the 1D system is due to the spin-charge separation inherent in the 1D

Mott insulators. We propose an effective model that can describe the optical nonlinearity, a *holon-doublon* model, where *holon* and *doublon* represent the charge degree of freedom for photo-induced unoccupied and doubly occupied sites, respectively. The model reproduces very well the characteristic behaviors of the experimental $\chi^{(3)}$.^{2,3} We find that the spin-charge separation becomes a key concept of future optoelectronic devices.

The electric field \mathbf{E} of the incident light induces the dielectric polarization \mathbf{P}_{ind} in a material, which is described by a power series of nonlinear optical susceptibility $\chi^{(n)}$: $\mathbf{P}_{\text{ind}} = \epsilon_0 (\chi^{(1)} \mathbf{E} + \chi^{(2)} \mathbf{E}^2 + \chi^{(3)} \mathbf{E}^3 + \dots)$. The linear susceptibility $\chi^{(1)}$ is given by

$$\chi_{jk}^{(1)}(-\omega; \omega) = \frac{1}{\epsilon_0 L} \frac{e^2}{\hbar} \sum_a \left(\frac{r_{0a}^j r_{a0}^k}{\Omega_a - i\Gamma_a - \omega} + \frac{r_{0a}^k r_{a0}^j}{\Omega_a + i\Gamma_a + \omega} \right), \quad (1)$$

where L is the number of sites, ϵ_0 is the dielectric constant, j and k are the polarization directions, er_{0a} is the dipole moment between the ground state $|0\rangle$ and excited state $|a\rangle$ with odd parity, Ω_a is the energy difference between $|0\rangle$ and $|a\rangle$, and Γ_a is the damping factor. Due to symmetry restrictions, $\chi^{(2)}$ vanishes in centrosymmetric materials to which Cu-oxides and Ni-halides belong. The lowest observable nonlinearity is, therefore, $\chi^{(3)}$, which is expressed as¹

$$\chi_{jklm}^{(3)}(-\omega_\sigma; \omega_1, \omega_2, \omega_3) = \frac{1}{\epsilon_0 L} \frac{e^4}{3! \hbar^3} \mathcal{P} \sum_{a,b,c} \frac{r_{0a}^j r_{ab}^k r_{bc}^l r_{c0}^m}{(\Omega_a - i\Gamma_a - \omega_\sigma)(\Omega_b - i\Gamma_b - \omega_2 - \omega_3)(\Omega_c - i\Gamma_c - \omega_3)}, \quad (2)$$

where $\omega_\sigma = \omega_1 + \omega_2 + \omega_3$, b and c denote even and odd states, respectively, and \mathcal{P} represents the sum of permutation on (j, ω_1) , (k, ω_2) , (l, ω_3) , and (m, ω_σ) . In the present study, by setting all of the polarization directions be the same along chains, we examine $\chi^{(3)}(-\omega; -\omega, \omega, \omega)$ and $\chi^{(3)}(-\omega; 0, 0, \omega)$, the imaginary

parts of which give two-photon absorption (TPA) and electroabsorption spectra, respectively. Hereafter, we set e , \hbar and ϵ_0 to be unity.

The insulating Cu-oxides and Ni-halides are known to be charge-transfer (CT)-type Mott insulators, where both $3d$ and $2p$ orbitals in the transition metal and ligand ions, respectively, participate in the electronic states. The values of the gap are predominantly determined by the energy position of the p orbitals. However, it is well established that the electronic states of the CT-type insulators can be described by the Hubbard model with single band by mapping a bound state called the Zhang-Rice singlet state onto the lower Hubbard band. Actually, the single-band Hubbard model explains very well spectral lineshape of angle-resolved photoemission and electron-energy loss spectroscopies in the insulating Cu-oxides.⁵⁻⁷

The single-band Hubbard Hamiltonian is defined as

$$H = -t \sum_{\langle i,j \rangle, \sigma} (c_{i,\sigma}^\dagger c_{j,\sigma} + \text{H.c.}) + U \sum_i n_{i,\uparrow} n_{i,\downarrow} + V \sum_{\langle i,j \rangle} n_i n_j, \quad (3)$$

where $c_{i,\sigma}^\dagger$ is the creation operator of an electron with spin σ at site i , $n_i = n_{i,\uparrow} + n_{i,\downarrow}$, $\langle i,j \rangle$ runs over pairs on nearest neighbor sites, t is the hopping integral, U is the on-site Coulomb interaction, and V is the Coulomb interaction between nearest neighbor sites.

The realistic values of the parameters for cuprates⁶⁻⁸ are chosen: $U/t=10$, and $V/t=1.5$ for 1D system and $V/t=1$ for ladder and 2D systems. Additionally, in the 2D system, a second-nearest neighbor hopping, t' , is considered to simulate a parent compound of high- T_c cuprates.^{6,8} The damping factors are assumed to be the same for all excited states of the systems with $\Gamma=0.4t$.⁹

We numerically examine linear absorption spectra, which are defined by an imaginary part of $\chi^{(1)}$, and TPA spectra for a 12-site chain with open boundary condition. The Lanczos technique is used for the calculation of the ground state. The spectra are calculated by using the correction vector technique.¹⁰ We also calculate them for two-leg ladder, and 2D systems with 12 sites in order to clarify the dependence of $\chi^{(3)}$ on dimensionality. The clusters used in the calculation are shown in Fig. 1 (c).¹¹

The calculated results are shown in Fig. 1(a) and (b). The solid, broken and dotted lines denote the results for the 1D, ladder and 2D systems, respectively. The upper panel (a) represents the linear absorption spectra, which detect odd states. The optical gap is estimated to ~ 2.4 ($=6t$) eV assuming $t \sim 0.4$ eV, comparable with the experimental optical gap.¹² The linear absorption has a large magnitude for the 1D system with strong enhancement in low-energy region ($\omega \sim 7t$), and decreases with increasing dimensionality from the 1D to 2D systems. These results are consistent with the experimental data of optical conductivity for 1D, ladder and 2D cuprates.¹²

The lower panel (b) shows the TPA spectra, which

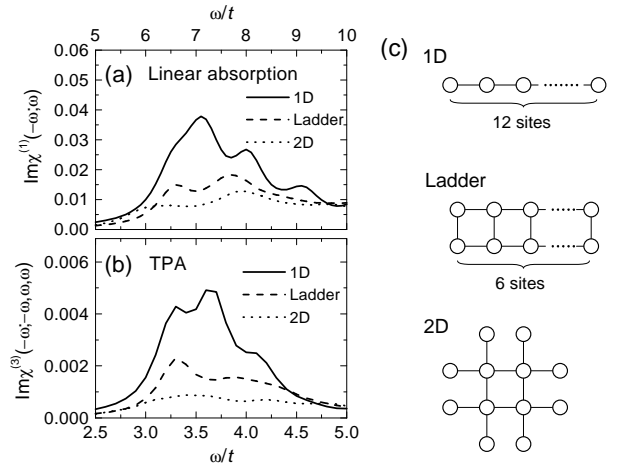


FIG. 1. The linear absorption (a) and TPA (b) spectra for the 1D, ladder and 2D Hubbard models, denoted by solid, broken and dotted lines, respectively. The clusters used in the calculation are shown in (c). $U/t=10$. $V/t=1.5$ for the 1D cluster and $V/t=1$ for the ladder and 2D clusters. For the 2D cluster, $t'/t=-0.4$.

detect even states with the same parity as the ground state. We find that the spectral shapes of TPA bear a close resemblance to those of $\chi^{(1)}$ when the energy in TPA is doubled. This means that the energy positions of the even states lie in the same energy region as the odd states shown in Fig. 1(a) (see the denominator of Eq. (2)).¹³ These characteristics are independent of the dimensionality, and agree with the results obtained by pump-probe measurements.^{3,4} We also find that the magnitude of $\chi^{(3)}$ is the largest in the 1D system, and decreases with increasing the dimensionality. This indicates that one-dimensionality is favorable to the enhancement of $\chi^{(3)}$, which is consistent with the recent experimental data on Sr_2CuO_3 and $\text{Sr}_2\text{CuO}_2\text{Cl}_2$.⁴

In order to clarify the TPA spectra in detail, we next examine photoexcited states and dipole moments between these states. The dipole moments are given by $\sum_i \langle \text{odd} | x_i n_i | \text{even} \rangle$, where $|\text{odd}\rangle$ and $|\text{even}\rangle$ denote eigenstates with odd and even parities for the Hamiltonian of Eq. (3), respectively, x_i is x -coordinate of the position at i site, and n_i is the number operator of electron.

Figure 2 shows the results of the energy distribution of dipole moments for the 1D (left panel) and 2D (right panel) systems, which are calculated exactly by using clusters shown in the insets. The upper panel [(a) and (d)] represents the dipole moments between the ground state and odd states. The middle panel [(b) and (e)] shows dipole moments between the first odd state labeled as O_1 in (a) and (d) and even states. In the 1D case, the O_1 state strongly couples to an even state with the nearly same energy as the O_1 state.^{13,14} The magnitude of the dipole moment is about 3. On the other hand, in the 2D case the dipole moment is smaller than that in the 1D system and the magnitude is less than 0.5. In

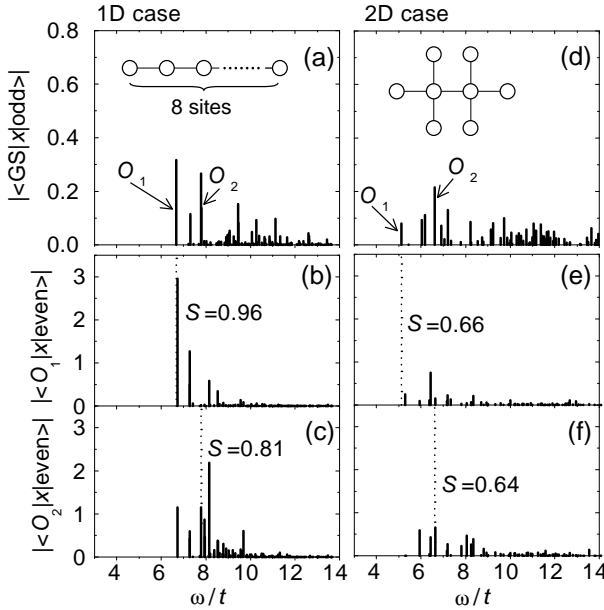


FIG. 2. The energy distribution of the dipole moments for 8-site 1D [(a), (b) and (c)] and 2D clusters [(d), (e) and (f)]. The (a) and (d) show the dipole moments between the ground state and the dipole-allowed states. The (b) and (e) ((c) and (f)) show the dipole moments between the dipole-forbidden states and typical two dipole-allowed states, denoted by O_1 (O_2) shown in (a) and (d). The S denotes a quantity to measure the similarity of the wavefunctions. $U/t=10$. $V/t=1.5$ for the 1D cluster and $V/t=1$ and $t'/t=-0.4$ for the 2D cluster.

addition, other dipole moments are also very small in the 2D system. The lower panel [(c) and (f)] shows dipole moments between another odd state O_2 and even states. We find again that an even state with very close energy to the O_2 state yields large dipole moment in the 1D case, whereas the dipole moment in the 2D case is small although there are even states whose energy is very close to the O_2 state. These results indicate a quantitative difference of the dipole moments between the 1D and 2D systems. The difference plays an important role in the difference of the magnitude of TPA between the 1D and 2D systems.

In general, the dipole moment becomes large when two states which lead to the dipole moment are constructed by similar wavefunctions. Therefore it is meaningful to examine the nature of the odd and even states in the 1D and 2D systems. We define a quantity S , which measures the similarity of the wavefunctions, as follows: $S \equiv \sum_i |\alpha_{o,i}\alpha_{e,i}|$, where $\alpha_{o,i}$ ($\alpha_{e,i}$) is the coefficient of a basis which constructs the odd (even) eigenstates of the Hamiltonian of Eq. (3), and i is the index of the bases. The quantity S becomes unity when two eigenstates are the same except for the phase of each basis.

In the 1D system, S between the O_1 (O_2) state and an adjacent even state is 0.96 (0.81), which is close to unity. On the other hand, in the 2D system, S is 0.66 and 0.64 for the O_1 and the O_2 states, respectively. These results

show that in the 1D system the two wavefunctions with close energies are quite similar each other in contrast to the 2D ones.

Next, we consider the origin of the different behavior of the photoexcited states between the 1D and 2D systems. In the 1D system, a photo-induced carrier separates into two collective modes carrying the spin and charge degrees of freedom (spin-charge separation). In addition, the wavefunction itself is factorized as the products of spin and charge wave functions when U is very large.¹⁵ Therefore, it is reasonable in the 1D system¹⁶ to take into account only the charge degree of freedom of electrons for the optical response. We propose below an effective model to describe the nonlinear optical response in the 1D system. In contrast to the 1D system, the motion of the carriers in the 2D system is known to be strongly influenced by spin background as long as the excitation energy is low,¹⁷ implying that the wavefunction cannot be simply factorized unlike the 1D system. It is, therefore, natural to suppose that the spin degree of freedom in the 2D system plays a crucial role in the broad spectral weight of $\chi^{(1)}$ and $\chi^{(3)}$ (Fig. 1) as well as the broad distribution of the photoexcited states (Fig. 2).

Based on the spin-charge separation picture, we introduce a *holon-doublon* model for the 1D Mott insulators. The Hamiltonian is given by

$$H = t \sum_i \left(h_i^\dagger h_{i+1} - d_i^\dagger d_{i+1} + \text{H.c.} \right) - V \sum_{\langle i,j \rangle} h_i^\dagger h_i d_j^\dagger d_j + \frac{U}{2} \sum_i \left(h_i^\dagger h_i + d_i^\dagger d_i \right), \quad (4)$$

with the constraint of no double occupation at site i , $(h_i^\dagger h_i + d_i^\dagger d_i) \leq 1$. The holon h (doublon d) represents the charge degree of freedom of unoccupied (doubly occupied) sites produced by the photoexcitation. We note that only two particles, i.e., one holon and one doublon, are contained in the present system. Although the model includes the attractive Coulomb interaction, we note that the model is different from a model for standard exciton of 1D semiconductors, since the holon and the doublon can not occupy the same site due to the hard core constraint unlike the semiconductors. As will be shown below, the constraint plays an important role in the degeneracy of the even and odd photoexcited states.

It is easily shown in the holon-doublon model that the even and odd states are degenerate and thus the overlap integral S between them is unity: Let us introduce a set of the bases with odd and even parities written as $|\text{basis}, o\rangle = (|hd00\dots\rangle - |00\dots dh\rangle)/\sqrt{2}$ and $|\text{basis}, e\rangle = (|hd00\dots\rangle + |00\dots dh\rangle)/\sqrt{2}$, where h , d and 0 denote holon, doublon, and vacant sites, respectively. Since there is no exchange between holon and doublon due to the hard core constraint, the first terms of the bases never couple to the second terms. This means that the matrix elements of the Hamiltonian of Eq. (4) are independent of the sign of the second terms. Therefore, the Hamiltonian matrix with odd parity is equal

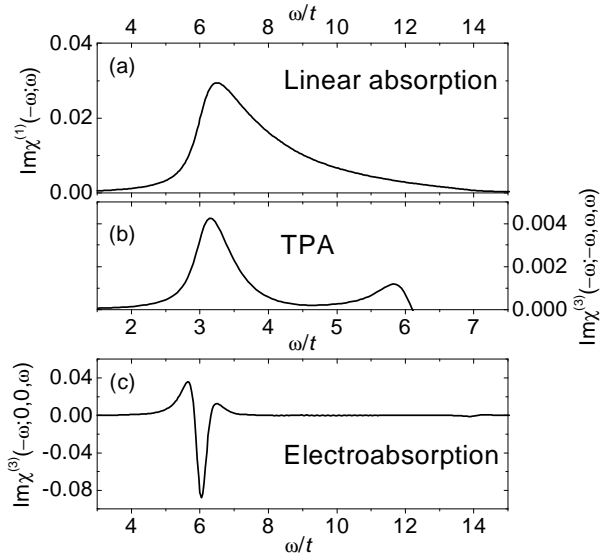


FIG. 3. The linear absorption (a), TPA (b) and electroabsorption (c) spectra obtained by holon-doublon model for a 80-site chain with open boundary condition. $U/t=10$, $V/t=1.5$ and $\Gamma/t=0.4$.

to that with even parity. This gives rise to the degeneracy between odd and even eigenstates and thus $S=1$. This model naturally explains the characteristics in the photoexcited states in the 1D Mott insulators discussed above. We note that the even and odd states are always degenerate regardless of the value of V (Ref. 17) or the range of Coulomb interactions.

Figure 3 exhibits the linear and nonlinear absorption spectra in the holon-doublon model for a 80-site chain.¹⁹ The linear absorption (a) and TPA (b) spectra reproduce well those for the 1D Hubbard model shown in Fig. 1. The obtained results are also very similar to those of the experimental data in Sr_2CuO_3 (Refs. 2 and 3) in the following points: (i) The spectral weights of linear absorption and TPA spectra are concentrated on the same energy region when the energy in TPA is doubled. (ii) The electroabsorption spectra (c) show an oscillating structure at the spectral edge of the linear absorption ($\sim 6t$). The agreement suggests that this model is a proper one in describing the nonlinear optical response in the 1D Mott insulators.

Finally we discuss the difference of nonlinear optical response between 1D band insulators and Mott insulators. The photoexcitation process in the band insulators creates an electron-hole pair bound by their attractive Coulomb interaction (Mott-Wannier exciton). The pair gives a series of bound states with odd and even parities below the gap. In fact, in the 1D band insulators such as silicon polymers²⁰ and Pt-halides,²¹ it has been observed that the odd and even states are concentrated on different energy regions, and their difference is rather large (~ 1 eV). However, such an energy difference between odd and even states is generally unfavorable for obtain-

ing the large dipole moments because dipole moments are inversely proportional to their energy difference. In this respect, the 1D Mott insulators are advantageous to large dipole moments since they have the nearly degenerate odd and even states as shown in Figs. 1 and 3, which leads to the large $\chi^{(3)}$.

In summary, we have clarified the nonlinear optical response and photoexcited states of Mott insulators. We found that $\chi^{(3)}$ is enhanced with decreasing the dimensionality, which is consistent with the recent experiments. In the 1D system, the odd and even photoexcited states are nearly degenerate in energy, and constructed by similar wavefunctions. We found that these properties, which become important for the large nonlinearity, are originated by the spin-charge separation. We also proposed the effective model in 1D Mott insulators. These findings imply that the novel concept of the spin-charge separation is not of purely academic interest but will show up in front of us as underlying physics of optoelectronic devices in the near future.

The authors thank H. Okamoto, H. Kishida, M. Kuwata-Gonokami and Y. Tokura for valuable discussions. This work was supported by a Grant-in-Aid for Scientific Research on Priority Areas from the Ministry of Education, Science, Sports and Culture of Japan, CREST and NEDO. The parts of the numerical calculation were performed in the supercomputing facilities of ISSP, University of Tokyo, and IMR, Tohoku University.

* To whom correspondence should be addressed.

E-mail address: tohyama@imr.tohoku.ac.jp

¹ See, for example, P. N. Butcher and D. Cotter, *The Elements of Nonlinear Optics* (Cambridge University Press, Cambridge, 1990).

² H. Kishida *et al.*, *Nature* **405**, 929 (2000).

³ T. Ogasawara *et al.*, *cond-mat/0002286*.

⁴ M. Ashida *et al.*, unpublished.

⁵ C. Kim *et al.*, *Phys. Rev. Lett.* **77**, 4054 (1996).

⁶ C. Kim *et al.*, *Phys. Rev. Lett.* **80**, 4245 (1998).

⁷ R. Neudert *et al.*, *Phys. Rev. Lett.* **81**, 657 (1998).

⁸ K. Tsutsui *et al.*, *Phys. Rev. Lett.* **83**, 3705 (1999).

⁹ The value of damping factor is unknown. However, the features of $\chi^{(1)}$ and $\chi^{(3)}$ discussed in the present work do not depend on the value.

¹⁰ Z. G. Soos *et al.*, *J. Chem. Phys.* **90**, 1067 (1989).

¹¹ No remarkable size dependence of $\chi^{(1)}$ and $\chi^{(3)}$ was observed between 8- and 12-site clusters.

¹² For example, see M. Imada *et al.*, *Rev. Mod. Phys.* **70**, 1039 (1998) for 1D cuprates, T. Osafune *et al.*, *Phys. Rev. Lett.* **78**, 1980 (1997) for ladder cuprates, and S. Uchida *et al.*, *Phys. Rev. B* **43**, 7942 (1991) for 2D cuprates.

¹³ In Ref. 3, the dipole moments and susceptibilities of the 1D two-band Hubbard model with $3d$ and $2p$ orbitals have been examined numerically for a finite-size ring. Their behaviors

reported are similar to those of the single-band Hubbard model discussed in the present work, although the concept of the spin-charge separation is not involved in Ref.3.

- ¹⁴ D. Guo *et al.*, Phys. Rev. B **48**, 1433 (1993).
- ¹⁵ M. Ogata and H. Shiba, Phys. Rev. B **41**, 2326 (1990).
- ¹⁶ W. Stephan and K. Penc, Phys. Rev. B **54**, R17269 (1996).
- ¹⁷ T. Tohyama *et al.*, J. Phys. Soc. Jpn. **69**, 9 (2000), and references therein.
- ¹⁸ If $V > 2t$, a bound state is formed for the total momentum $K = 0$ (Ref. 16).
- ¹⁹ We note that the ground state of this model is a vacuum without holon and doublon. The details of the calculation of $\chi^{(1)}$ and $\chi^{(3)}$ will be shown elsewhere.
- ²⁰ T. Hasewgawa *et al.*, Phys. Rev. Lett. **69**, 668 (1992).
- ²¹ Y. Iwasa *et al.*, Appl. Phys. Lett. **59**, 2219 (1991).